

# Influence of Exposure Guidelines on the Design of On-Body Inductive Power Transfer

Lindsay Clare, Paul Worgan, Bernard H. Stark, Salah-Eddine Adami, David Coyle  
Faculty of Engineering, University of Bristol, Bristol, United Kingdom

**Abstract**—Designers of on-body health sensing devices with inductive power transfer (IPT) face a number of trade-offs. Safe exposure limits should be maintained, and protective housing and padding are generally needed; however, these impose compromises on the power-transfer-system design. This paper analyses these trade-offs and proposes a design route to achieving high power transfer in the presence of field restrictions and separations for padding or housing materials. An IPT system using a Class D coil-driver and switched-mode power-conditioning is designed to provide regulated d.c. and energy storage. Compliance with ICNIRP 1998 guidelines is demonstrated, at a power level that is sufficient to power typical on-body medical sensing devices.

**Keywords**—on-body sensing, inductive power, wireless power transfer, healthcare.

## I. INTRODUCTION

There is an ever increasing number of studies by groups who are developing on-body sensors for healthcare and activity monitoring. Typically, these sensors should not play a prominent role in a person's day-to-day routine, and therefore inductive power transfer is seen as an important option for the supply of power. Inductive power transfer is already employed in the medical field to power implanted sensors and devices. Inductive power transfer to wearables has also received interest [1].

While closely coupled inductive power transfer, for example for vehicle charging, achieves high transfer efficiencies, on-body sensors impose additional challenges and constraints on inductive power transfer. Firstly, human exposure to magnetic fields should be limited: devices for use in Europe have to comply with safe exposure guidelines published by the International Commission on Non-Ionizing Radiation Protection (ICNIRP) [2]. These guidelines currently represent the most stringent international guidelines and are thus adopted in this paper. They impose frequency-dependent limits on tissue currents, which result in a limitation on the useable peak magnetic field strength. Secondly, the mechanics of on-body sensing, and the requirement for a system that is safe for people's daily routine, requires a system topology that maintains safe exposure under all circumstances. In practice this leads to the use of safety padding, as illustrated in Figure 1. This affects the coupling of the system and influences the potential power transfer.

Thirdly, and because people's routines can vary widely, contact cannot be guaranteed, and the system's normal use is under changing loose coupling, with a significant transmitter-receiver spacing  $Y_S$ .

This paper makes several contributions. First, we show the impact of developing an on-body inductive power transfer system to be compliant with the ICNIRP guidelines on

electromagnetic energy exposure [2]. Second, a driver circuit for loose coupled transfer is presented, and its performance established.

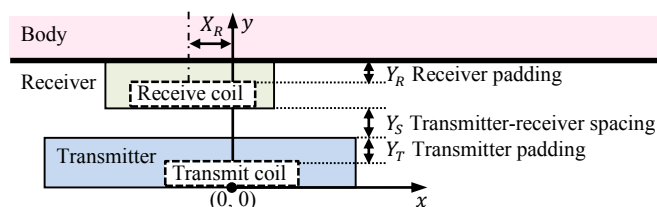


Figure 1: On-body inductive power transfer working scenario, showing definitions of parameters and axes.

Overall, this paper demonstrates that it is feasible to design on-body sensors that use non-contact inductive charging, thus enabling more continuous sensing, whilst adhering to the most stringent international safety guidelines and also delivering devices that are wearable and provide sufficient power for use in a wide variety of on-body sensors and healthcare systems.

## II. INDUCTIVE POWER SYSTEM

The receive coil and power conditioning circuit are on the user's body. The receive coil is positioned on the body in such a way as to interact with the transmit coil embedded within the user's environment. For an explanation of the theory of coupled-tuned circuits as used here, see [3]. A frequency of 100 kHz was chosen, as designing for compliance to human exposure limits above this frequency is far less straightforward.

Commercially available coils were used; part of the Seed Studio POW0114B wireless charging module, as they had suitable dimensions and were designed for operation at frequencies similar to those investigated here. They have the following measured specification:

Mean radius:	17 mm
Height:	1.65 mm
Winding:	25 turns, 0.45 mm diameter
Inductance:	30.6 $\mu$ H
DC resistance:	0.25 $\Omega$
AC resistance:	approx. 1 $\Omega$ at 100 kHz
Q-factor:	approx. 19 at 100 kHz

A high Q-factor is desirable, as it improves power-transfer in loosely-coupled circuits [4]. It is equal to the ratio of inductive reactance to a.c. resistance of the coil. The a.c. resistance at this frequency may be reduced by winding with multi-stranded enamelled wire (Litz) to reduce skin-effect [5].

The transmit-coil is driven in series resonance by a Class D half-bridge circuit, as shown in Figure 2. Q1 and Q2 are driven alternately, switching one end of the series circuit between V+

and ground, the other end being held at mid-rail potential by C4 and C5. A 100 kHz square-wave voltage with peak amplitude of  $V+2$  is thereby applied to the circuit, which being resonant at 100 kHz, is selective at the fundamental frequency, resulting in a sinusoidal transmit coil current.

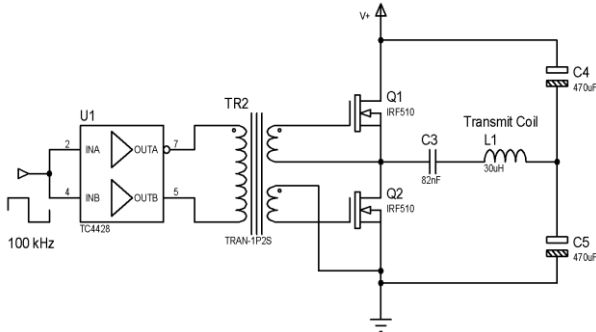


Figure 2: Half-bridge coil-driver circuit.

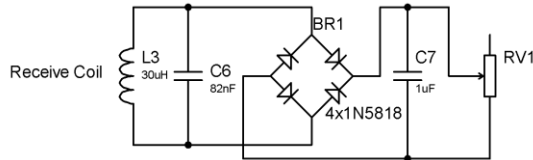


Figure 3: Receive-coil test-circuit.

The receive-coil test circuit is shown in Figure 3. It is parallel-tuned by C6 to 100 kHz: the output is rectified and smoothed by C7 and loaded by a variable resistance. In a practical system the resistive load would be a flyback converter operating in discontinuous mode with shunt-regulated output. This would provide regulated d.c. with energy storage and present the receive coil with the required resistive load [6].

The voltage induced into the secondary circuit is proportional to the rate of change of flux linkage, which depends on the amplitude and frequency of the transmit-coil current at a given coil spacing. Increasing the amplitude and frequency of the transmit coil current increases the peak field gradient and thereby also the receive coil voltage. This increase is not unlimited however: ICNIRP guidelines limit the magnetic field strength magnitude as a function of frequency. These limits form the basis of the design method presented here.

### III. NON-IONIZING RADIATION PROTECTION LIMITS

Equation (1) (Eqn. 4 of the ICNIRP 1998 guidelines [2]), and the transformer Equation (2) are used to determine the inductive power transfer systems compliance with the ICNIRP 1998 guidelines. Using (1), the ICNIRP 1998 guideline value for current density  $J$  can be converted to a guideline magnetic flux density  $B$  when the transmit coil radius  $R$ , tissue conductivity  $\sigma$ , and frequency  $f$ , are known.

$$J = \pi R f \sigma B \quad (1)$$

$$V_{RMS} = 4.44 A B_{Peak} N f \quad (2)$$

In (1) we assume a homogenous conductivity for human muscle tissue, having a value of 0.362 S/m at 100 kHz. Using (1) and substituting in the maximum permissible value for  $J$  at 100 kHz of 0.2 A/m<sup>2</sup> and a mean coil radius of 17 mm, the maximum magnetic flux density allowable at the tissue surface is 103.4  $\mu$ T rms or 146.2  $\mu$ T peak. The flux density at the tissue

surface may be determined by measuring the voltage  $V_{RMS}$  across a search-coil, and substituting the number of turns  $N$  and the mean turn-area  $A$  into (2).

### IV. DESIGNING AN ON-BODY INDUCTIVE POWER TRANSFER SYSTEM

In order to meet the most stringent international guidelines and for operation in Europe, design of an IPT system is largely driven by the need to comply with ICNIRP guidelines, which for the size of coil used here fixes the maximum flux exposure level to 103.4  $\mu$ T rms, as shown above. It might be thought that to obtain maximum power transfer between the two coils, the transmit coil would be placed flush with the surface, minimising the distance between the coils, thereby maximising the coupling factor. However, where tuned-coupled-circuits are used, power transfer to the receive coil does not increase monotonically as the coils are brought closer together, but reaches a maximum at some intermediate spacing (critical coupling) [3], and falls rapidly as the coils close up. Therefore the transmit coil is set below the surface at a distance shown as  $Y_T$  in Figure 1, which may need to be a compromise between physical constraints and optimum performance. The transmit-coil current is adjusted to give 100  $\mu$ T at the surface, measured using a search-coil. This ensures a safe level of exposure with the receive-coil removed, but when the resonant receive coil is brought towards the surface, it concentrates the flux in the area around it, potentially bringing it far above the safe level at the body. This can be controlled in two ways; by introducing padding between the receive coil and body, and by varying the load resistance. Up to a point, increasing load resistance increases power, but due to reduced damping on the tuned circuit, requires thicker padding. This is shown in Figure 4 and Figure 5, taken with the coils coaxially aligned. These plots illustrate the interdependencies in the system. For these tests, the receive-coil was parallel-tuned to 100 kHz and connected via a full-wave rectifier to a decade resistance box and smoothing capacitor. The procedure for constructing these plots was:

1. Using a search-coil, set the transmit-coil current to give a flux density of 100  $\mu$ T for the chosen transmitter padding thickness  $Y_T$ , i.e. at the surface.
2. For each value of receiver padding thickness  $Y_R$ , set the load resistance to give 100  $\mu$ T at the body, measured using a search-coil, and calculate the load power.

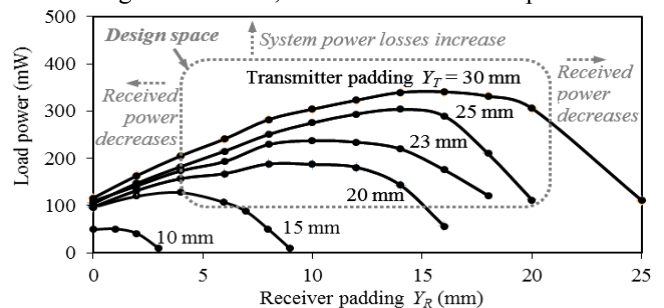


Figure 4: Power delivered to load against receiver padding  $Y_R$  (as defined in Figure 1), with transmitter padding  $Y_T$  as a parameter, where a magnetic flux density of 103.4  $\mu$ T rms is maintained at the body. Coil axes are aligned.

Whilst these power curves illustrate the general trend of inductive power transfer systems, Figure 4 and Figure 5 have been specifically plotted for a  $B_{RMS}$  of 103.4  $\mu$ T. If the transmit

coil geometry is changed, then a new value of  $B_{RMS}$  would apply and a new set of power curves would have to be plotted. The designer could then follow our design procedure with their new system.

In practice, the dimensions of  $Y_T$  and  $Y_R$  will probably be constrained by what is physically convenient in a particular setting, e.g. 5 mm may be a maximum for receiver padding to allow people to comfortably wear an inductively charged sensor, and the transmit-coil can only be sunk a maximum of 25 mm below a surface such as a table or arm rest. From Figure 4 this gives a load power of 160 mW, and reference to Figure 5 shows that a load resistance of approximately 150  $\Omega$  is required.

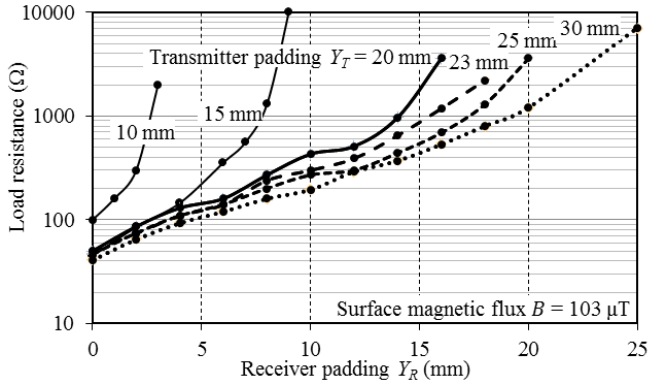


Figure 5: Load resistance that maintains a magnetic flux density of 103.4  $\mu\text{T}$  at the body, against receiver padding  $Y_R$ , with transmitter padding  $Y_T$  as a parameter.

## V. EXPERIMENTAL RESULTS

Figures 6-8 illustrate the ICNIRP compliance of our system in a range of safety critical scenarios that are envisaged. Figure 9 shows the effect of coil misalignment on load power.

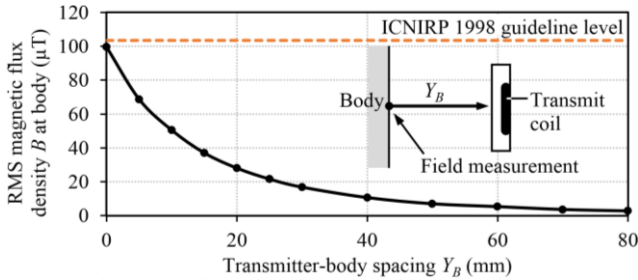


Figure 6: Measured RMS magnetic flux density  $B$  at the body, against spacing between transmitter and body  $Y_B$  with no receiver present.

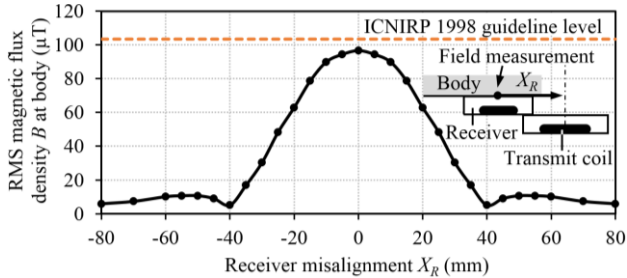


Figure 7: Measured RMS magnetic flux density  $B$  against receiver coil misalignment  $X_R$ . Search coil on receive coil axis.

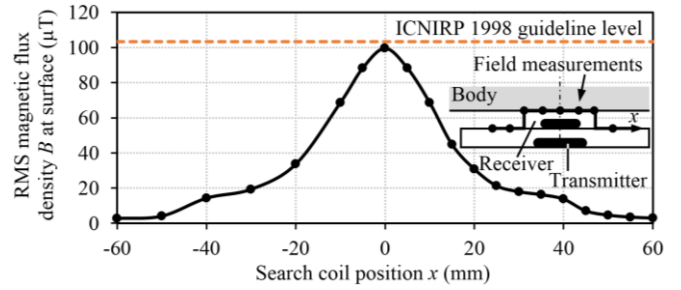


Figure 8: Measured RMS magnetic flux density  $B$  against  $x$ -position along accessible surfaces. Coils aligned, and minimum transmitter-receiver spacing.

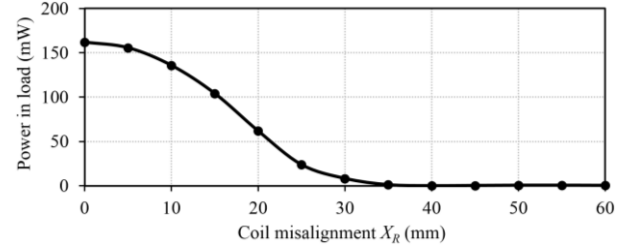


Figure 9: Variation of power in load against coil misalignment  $X_R$ .  $Y_T=23\text{mm}$ ,  $Y_R=5\text{mm}$ .

## VI. POWER CONDITIONING

In this work, the target application is a wearable 3-axis accelerometer incorporating a microprocessor and radio transmitter. The device operates over an input voltage range of 2.3 V to 6 V, an on-board buck regulator providing 1.8 V for the active circuits. Figure 5 implies that the voltage at the output of the IPT system determines the level of magnetic flux at the body surface and so must be limited. In the above tests, this was achieved by loading with a decade resistance box connected across the output of the rectifier, which simply dissipated the power. However, we wish to transfer the power to a load, yet still provide a fixed load resistance for the IPT system. This may be achieved by the use of a type of switched-mode converter, sometimes known as a resistance emulator, which provides a fixed resistance at the input over a range of load conditions on the output side. Switched-mode regulators are available that work efficiently at the low power levels used here, but are not suitable as they utilize a voltage feedback loop to provide output regulation, resulting in a negative input resistance. Since these feedback arrangements cannot usually be circumvented easily, we make recourse to a bespoke design in the form of a flyback converter operating in discontinuous inductor current mode (DCM), the principles of which are described in [6]. This type of converter emulates a resistance at its input which may be set to the required value by means of PWM duty-cycle adjustment: it follows the rectifier shown in Figure 3, taking the place of the load resistor. Taking values for  $Y_T$  and  $Y_R$  of 25 mm and 5 mm respectively, the required resistance is 150  $\Omega$  and the power, 160 mW. The converter is shown in schematic form in Figures 10 and 11.

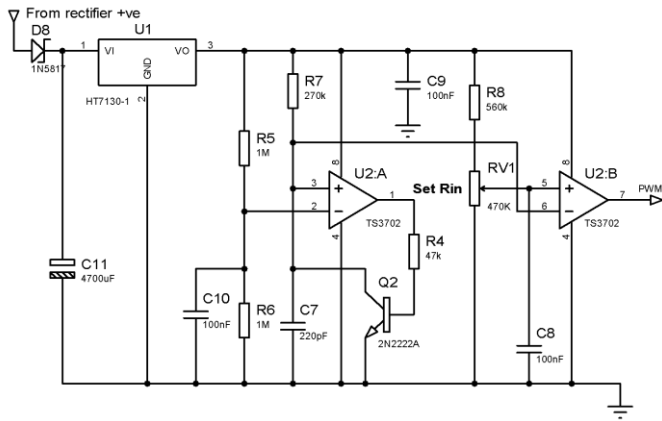


Figure 10. Flyback converter PWM generator.

Figure 10 shows the PWM generator circuit; it is supplied with 3.3 V from the IPT system via LDO U1. C11 provides a measure of hold-up power such that the converter can continue to operate when the coils shift to a less favourable position. A switching frequency of 25 kHz rather than the more usual 100 kHz or higher is chosen to reduce the power overhead of the PWM waveform generator to a small proportion of the power throughput. U2 is a dual micropower comparator with U2a operating as a relaxation oscillator providing a ramp waveform to PWM comparator U2b. The PWM duty-cycle is variable by means of RV1 and this sets the input resistance which is given by

$$R_{in} = \frac{2L}{D^2T} \quad (3)$$

where L is the primary inductance of TR1 and T is the switching period.

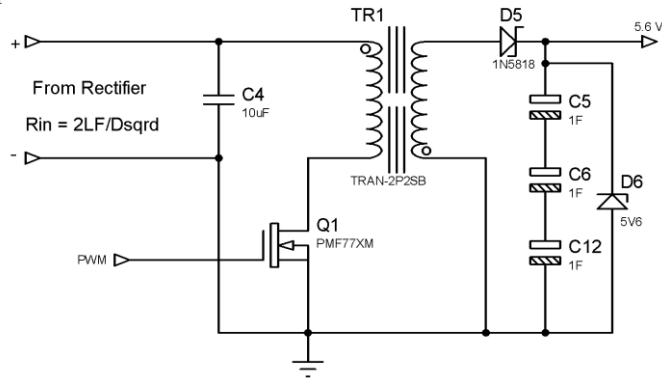


Figure 11. Flyback converter power section.

Figure 11 shows the converter power section. The PWM waveform from U2b drives MOSFET Q1 in a conventional flyback stage which charges supercapacitors C5, C6 and C12. Zener diode D2 limits the charging voltage to 5.6 V, which is stepped down to 1.8 V by the buck converter on the accelerometer board. The converter only operates as a resistance emulator in discontinuous mode and therefore the design must ensure that the boundary to continuous mode is not crossed under normal operating conditions. The worse-case condition is at maximum input power and minimum input voltage. For this

system these values are 0.16 W and 4.9 V respectively. Although  $V_{out}$  will normally be 5.6 V, it is desirable that discontinuous operation is maintained at lower voltages when the supercapacitor is only partially charged, and so a minimum for  $V_{out}$  of 2.5 V is chosen. It can be shown that the value of inductance that puts the converter on the borderline between continuous and discontinuous mode is given by

$$L_{crit} = \frac{(V_{in}V_{out})^2 T}{2P_{in}(V_{out} + nV_{in})^2} \quad (4)$$

Where  $n$  is the turns ratio of the flyback transformer  $N_s/N_p$ . Substituting these values into Equation 4 and using a one-to-one turns ratio, gives an inductance value of 340  $\mu$ H. From Equation 3, the required duty-cycle for an input resistance of 150  $\Omega$  is found to be 0.34.

With an input power of 160 mW and with the output shunt regulated at 5.6 V, the power output to the shunt regulator was 143 mW, indicating an efficiency of 89.4 %. The 0.33 F supercapacitor charged to 5.6 V in 43 seconds. This is approximately 7 seconds longer than would be calculated for a constant charging power of 143 mW, but is explained by the fact that at the start of the charging period, the converter is in continuous mode, changing to DCM at 2.35 V, and that the sensor board is also drawing power through the charging period.

## VII Conclusions.

We have shown how to develop and deploy an ICNIRP 1998 guideline compliant on-body inductive power transfer systems for wearable health sensing. The design spaces and effect on the power delivered to the load resistor associated with geometric design choices have been discussed. A power-conditioning system providing a fixed load to the IPT system with regulated output voltage has been shown.

## ACKNOWLEDGEMENTS

This work was performed under the SPHERE IRC funded by the UK Engineering and Physical Sciences Research Council (EPSRC), Grant EP/K031910/1.

## REFERENCES

- [1] O. Jonah, S. Georgakopoulos, and M. Tentzeris, "Wireless power transfer to mobile wearable device via resonance magnetic," in *Wireless and Microwave Technology Conference (WAMICON), 2013 IEEE 14th Annual*, April 2013, pp. 1–3.
- [2] "ICNIRP guidelines for limiting exposure to time-varying electric and magnetic fields (1Hz - 100kHz)," *Health Physics*, vol. 74, no. 4, pp. 494–522, April 1998.
- [3] Terman F. E. *Electronic and Radio Engineering*. McGraw-Hill Book Company Inc. 1955. pp 63-70.
- [4] Design and Optimization of Circular Magnetic Structures for Lumped Inductive Power Transfer Systems. Mickel Budhia, Grant A. Covic and John Boys. *IEEE Transactions on Power Electronics*. Vol. 26, No. 11, November 2011.
- [5] J.H. Morecroft. Resistance and capacitance of coils at radio frequencies. *IRE*, Vol 10, 1922, pp 261-286.
- [6] S. Burrow and L. Clare, "Open-loop power conditioning for vibration energy harvesters," *Electronics Letters*, 45(19), 999–1000, 2009.